Non-conventional serine protease activity of the CXC chemokine-cleaving streptococcal enzyme, SpyCEP

Max Pearson[1,2], Carl Haslam[3], Andrew Fosberry[3], Emma J Jones[3], Mark Reglinski[1] , Robert J. Edwards[4], Richard Ashley Lawrenson[1], Danuta Mossakowska[3,5], James Edward Pease[6], Shiranee Sriskandan[1, 2]

[1]Department of Infectious Disease, Imperial College London, London W12 0NN, UK

[2]MRC Centre for Molecular Bacteriology & Infection, Imperial College London, London, SW7 2AZ, UK

[3]GlaxoSmithKline R&D, Gunnels Wood Road, Stevenage, Hertfordshire, SG1 2NY, UK

[4]Department of Medicine, Imperial College London, W12 0NN, UK

[5]Malopolska Centre of Biotechnology, Jagiellonian University, 30-387 Kraków, Poland

[6]National Heart and Lung Institute, Imperial College London, London, SW7 2AZ, UK

Character count: 46516

Abstract

The *Streptococcus pyogenes* cell envelope protease (SpyCEP) is a vital virulence factor in streptococcal pathogenesis. Despite its key role in disease progression and strong association with invasive disease, little is known about the enzymatic function beyond the ELR^+ CXC chemokine substrate range. We utilised multiple SpyCEP constructs to interrogate the protein domains and catalytic residues necessary for enzyme function. We leveraged high-throughput mass spectrometry to describe the Michaelis-Menton parameters of active SpyCEP, revealing a Michaelis-Menton constant (K_M) of 53.49 nM and a turnover of 1.34 molecules per second, for the natural chemokine substrate CXCL8.

Unexpectedly, we found that an N-terminally-truncated SpyCEP C-terminal construct consisting of only the H279 and S617 catalytic dyad had specific CXCL8 cleaving activity, albeit with a reduced substrate turnover of 2.45 molecules per hour, representing a ~2000-fold reduction in activity. In contrast, the K_M of the C-terminal SpyCEP construct and full-length enzyme did not differ. We conclude that the SpyCEP C-terminus plays a key role in substrate binding and recognition with key implications for both current and future streptococcal vaccine designs.

Word count: 175

59 **Introduction**
60

61 Group A Streptococcus (GAS) or *Streptococcus pyogenes* is a leading human pathogen that
62 manifests clinically as a broad spectrum of diseases, ranging from less severe, usually self-limiting
63 infections to life-threatening invasive diseases such as necrotizing fasciitis and toxic shock syndrome.
64 While much of the global health burden can be attributed to streptococcal auto-immune sequelae
65 such as rheumatic heart disease, invasive diseases contribute greatly to *S. pyogenes* associated
66 global mortality. Invasive infections account for an estimated 163,000 deaths worldwide per year
67 and at least 663,000 new cases (Carapetis et al., 2005) with mortality rates remaining high despite
68 intervention; indeed, 20% of patients with invasive *S. pyogenes* disease die within 7 days of infection
69 (Ralph and Carapetis, 2013).

70 Several virulence factors contribute to pathogenesis in invasive *S. pyogenes* disease, chief
71 among which is *Streptococcus pyogenes* cell envelope protease (SpyCEP), an immune-modulatory
72 cell wall-associated protease. SpyCEP is responsible for the rapid and efficient cleavage of a distinct
73 group of CXC chemokines comprising CXCL1, CXCL2, CXCL3, CXCL5, CXCL6, CXCL7 and CXCL8 both
74 locally at the site of an infection, and systemically, (Edwards et al., 2005, Kurupati et al., 2010,
75 Turner et al., 2009a, Zingaretti et al., 2010). The ELR^+ chemokines, named for their conserved N-
76 terminal glutamate- leucine- arginine motifs, specifically act upon neutrophils eliciting their
77 recruitment and activation. SpyCEP inactivates these chemokines by cleaving the chemokine C-
78 terminal α-helix, releasing a 13 amino acid peptide in the case of CXCL8 (Edwards et al., 2005).
79 Specificity for binding the neutrophil chemokine receptors CXCR1 and CXCR2 is conferred to a large
80 extent by the chemokine N-terminal ELR motif (Middleton et al., 1997), although the chemokine C-
81 terminus is necessary for efficient receptor binding and activation (Goldblatt et al., 2019) in addition
82 to chemokine translocation from tissues to endothelial lumen (Middleton et al., 1997). As such,
83 SpyCEP cleavage of CXC chemokines results in a reduction of CXCR1 and CXCR2-mediated neutrophil
84 chemotaxis and subsequent paucity of neutrophils at the site of *S. pyogenes* infection (Edwards et
85 al., 2005). In addition to CXC chemokines, SpyCEP has recently been shown to cleave the human

86 anti-microbial peptide, LL-37 (Biswas et al., 2021). Whilst cleavage does not affect the antimicrobial
87 action of the peptide, it was reported to reduce LL-37 specific neutrophil chemotaxis (Biswas et al.,
88 2021).

89 SpyCEP is expressed by *S. pyogenes* as a 1647 amino acid, 180 kDa subtilisin-like serine
90 protease, the crystal structure of which was recently solved to 2.8 Å resolution (Jobichen et al.,
91 2018) and further refined to 2.2 Å resolution (McKenna et al., 2020). It is a member of the S8
92 subtilase family, members of which are characterised by a catalytic triad consisting of an aspartate,
93 histidine and serine residue each surrounded by a region of highly conserved amino acids (Siezen,
94 1999). SpyCEP is unique among streptococcal proteases in that, during maturation, it is
95 autocatalytically cleaved between residues Q244 and S245 into 2 distinct polypeptides, a 30 kDa N-
96 terminal polypeptide and a 150 kDa C-terminal polypeptide. The two polypeptides harbour the
97 separate residues required for the formation of the catalytic site (Zingaretti et al., 2010); the N-
98 terminal fragment contains the catalytic D151 and the C-terminal fragment contains the catalytic
99 H279 and S617 residues. Upon cleavage, the two polypeptides re-associate non-covalently to
100 reconstitute the active enzyme (Zingaretti et al., 2010). The recent crystal structures have shed
101 further light upon the structure of SpyCEP, describing 9 separate domains, the first 5 of which
102 contain the catalytic triad necessary for enzymatic activity (Jobichen et al., 2018).
103 SpyCEP has been included as a target antigen in several recent *S. pyogenes* vaccine designs due to its
104 cell surface expression, highly conserved nature, and central role in *S. pyogenes* pathogenesis.
105 Immunisation with SpyCEP successfully elicits a SpyCEP-specific neutralising antibody response,
106 providing protection against systemic bacterial dissemination and reducing disease severity in *S.*
107 *pyogenes* intramuscular, skin infection models and non-human primate infection models (Rivera-
108 Hernandez et al., 2019, Bensi et al., 2012, Pandey et al., 2015, Pandey et al., 2016, Rivera-Hernandez
109 et al., 2016, Turner et al., 2009b). Data that demonstrate vaccine dependence on enzyme inhibition
110 highlight the importance of understanding the enzymatic activity of SpyCEP and the potential to
111 improve upon vaccine or inhibitor design.

112 Despite this, little is known about the catalytic properties of the enzyme, except preliminary
113 structure-function studies (Kaur et al., 2010, Jobichen et al., 2018, McKenna et al., 2020, Zingaretti et
114 al., 2010). Published data largely focuses on the impact of SpyCEP on streptococcal pathogenesis and
115 disease progression. In this study we generated multiple SpyCEP constructs to confirm domains
116 necessary for catalytic activity. We then used mass spectrometry to determine the enzyme kinetics
117 of multiple SpyCEP constructs for the natural substrate CXCL8 .

118 **Methods**

119 **Cloning and purification of recombinant SpyCEP constructs**

120 Codon-optimized SpyCEP gene constructs were expressed in *Escherichia coli* using synthetic gene
121 sequences (GenScript) from Spy_0416 in the SF370 *S. pyogenes* M1 genome (Abate et al., 2013,
122 Zingaretti et al., 2010) representing full-length enzyme, SpyCEP$^{34\text{-}1613}$, the N- terminal polypeptide,
123 SpyCEP$^{34\text{-}244}$, and C-terminal polypeptide SpyCEP$^{245\text{-}1613}$. Constructs were also generated with alanine
124 substitutions to replace catalytic residues in the N-terminal fragment (SpyCEP$^{34\text{-}244}$ D151A), and the
125 C-terminal fragment (SpyCEP$^{245\text{-}1613}$ S617A). To enable downstream protein purification, both the
126 full-length enzyme and C-terminal polypetides were synthesized with a C-terminal 6X-Histidine tag
127 and the N-terminal polypeptides were synthesized with an N-terminal FLAG tag and TEV linker.

128 All SpyCEP constructs were cloned into the vector pET-24B and expressed in BL21 (DE3) competent
129 *E. coli*, cultured in Terrific Broth (TB) medium supplemented with 50 µg/mL kanamycin at 37°C, 200
130 rpm, for 3 hours. The cultures were induced with 0.5 mM Isopropyl β-D-1-thiogalactopyranoside
131 (IPTG), cooled to 15°C and incubated at 200 rpm for 16 hours before lysis by sonication on ice. Full-
132 length and C-terminal contructs were purified by Ni-IDA affinity chromatography (GenScript) as per
133 the manufacturer's instructions. N-terminal constructs were purified by anti-flag M2 agarose resin
134 chromatography (Sigma-Aldrich, A2220) as per manufacturers instruction, and further concentrated
135 and purified by SP ion-exchange (Sigma-Aldrich, 17-1152-01) and Q FF ion-exchange
136 chromatography (GE Healthcare, 17-5156-01) as per manufacturer's instruction. All SpyCEP

137 constructs were subsequently concentrated and purified by size exclusion chromatography on a
138 HiLoad Superdex 200 or 75 prep grade column (GE Healthcare) dependent on molecular weight.

139 The resultant panel of recombinantly expressed SpyCEP constructs is shown in Table 1. The re-
140 association of the SpyCEP N and C-termini to create full-length constructs was carried out by
141 equimolar co-incubation at 37°C for 30 minutes in 40 mM Tris-HCL pH 7.5, 0.1 mM CHAPS, 1 mM
142 DTT, 0.1% BSA, 75 mM NaCl.

143

144 **Table 1. SpyCEP constructs used in this study.** Constructs were expressed recombinantly in *E. coli*
145 except for s.pSpyCEP that was expressed in, and purified from *S. pyogenes* .

146

147 **Construction of recombinant *S. pyogenes* expressing histidine-tagged SpyCEP**
148

149 To permit release of soluble His-tagged SpyCEP by *S. pyogenes*, the C-terminal anchor domain of
150 SpyCEP was replaced by a stop codon in strain H292, a strain that makes abundant SpyCEP (Turner et
151 al., 2009a). A 549 base pair region immediately upstream of the SpyCEP cell wall anchor motif was
152 amplified from *S. pyogenes* H292 genomic DNA using the primers
153 :5'GGGAATTCTGTTGTCAGGTAACAGTCTTATCTTGCC -3' and
154 5'CCGAATTCACAACACTAGGCTTTTGCTGAGGTCGTTG -3'. *EcoRI* restriction sites were incorporated at
155 the terminal ends of the primer sequences. The amplified DNA was cloned into the homologous
156 recombination plasmid pUCMUT to produce the vector pUCMUT$_{CEP}$ which was transformed into One
157 Shot TOP10 Chemically Competent *E. coli* (Thermo Fisher Scientific) according to the manufacturer's
158 instructions. The nucleotide sequence of the SpyCEP C-terminus was subsequently further modified
159 to encode a hexa-histidine tag by inverse PCR using pUCMUT$_{CEP}$ as the template and the primers 5'-
160 TATCCTAGGTAGTGTTGTGAATTCGTAATCATGGTCATAG-3' and 5'-
161 TATCCTAGGATGATGATGATGATGATGGGCTTTTGCTGAGGTCGTTG-3'. The amplification was
162 preformed using GoTaq Long PCR Master Mix (Promega) according to the manufacturer's
163 instructions. *AvrII* restriction sites, incorporated at the terminal ends of the primer sequences,

164 facilitated re-circulation of the amplified plasmid. The presence of a hexa-his sequence in the
165 modified $pUCMUT_{CEP}$ construct (denoted $pUCMUT_{CEP-HIS}$) was confirmed by Sanger sequencing using
166 the pUCMUT sequencing primers 5'- GACAGCAACATCTTTGTGAAAGATGG-3' and 5'-
167 CATTAATGCAGCTGGCACGAC-3'. The $pUCMUT_{CEP-HIS}$ construct was introduced into H292 by
168 electroporation and crossed into the chromosome by homologous recombination as previously
169 described (Lynskey et al., 2013) to generate strain H1317. Secretion of His- tagged SpyCEP into the
170 culture supernatant of H1317 was confirmed by western blotting (data not shown). To purify
171 SpyCEP, *S. pyogenes* H1317 was grown in Todd-Hewitt broth (Oxoid) overnight at $37^{o}C$ with 5% $C0_2$
172 The culture was pelleted at 2500 xg for 10 minutes and the supernatant sterilised using Amicon 0.22
173 µM filters, then concentrated using 15 ml Amicon 100 kDa centrifuge filter columns and purified by
174 nickel column affinity chromatography (Novagen His-Bind Resin) as per the manufacturer's
175 instructions.

176

177 **Sodium dodecyl sulphate–polyacrylamide gel electrophoresis (SDS-page)**

178 To visualise chemokine cleavage, 5 µM recombinant human CXCL1 and CXCL8 (R&D Systems) was
179 incubated with full-length recombinant SpyCEP or C-terminal SpyCEP at a molar ratio of 1:5, 50, 500,
180 5000 in favour of chemokine for 2 hours at $37^{O}C$. $SpyCEP^{DASA}$, C-terminal^{SA} and N-terminal
181 constructs$^{34-244}$ were included as controls and assayed at the highest 1:5 molar ratio. Reactions were
182 halted by the addition of Dithiothreitol (DTT) to a final concentration of 100 mM, 4X Bolt LDS sample
183 buffer and heating to 70°C for 10 minutes. Samples were separated on pre-cast 4-12% MES buffered
184 Bolt Bis-Tris gradient gels (Invitrogen) by SDS-PAGE gel electrophoresis at 165 V for 35 minutes with
185 SeeBlue Plus 2 (Invitrogen) used for molecular weight ladder. Gels were stained with PageBlue
186 protein staining solution (Thermo Fisher Scientific) overnight and de-stained in deionised water.

187

188 **Multiplex fluorescent western blotting**

189 To visualise generation of both intact CXCL8 and the larger (N-terminal) CXCL8 cleavage product, a
190 rabbit antiserum was raised against the neo-epitope (anti-ENWVQ) that is exposed following SpyCEP
191 cleavage of CXCL8 (Edwards et al., 2007). SpyCEP constructs were incubated at 37 °C with 937.5 nM
192 of recombinant human CXCL8 (R&D Systems) at a 1:50 molar ratio in favour of CXCL8. Digests were
193 halted and separated by SDS-PAGE gel electrophoresis as described above. Proteins were
194 transferred by iBlot2 (Thermo Fisher Scientific) onto 0.22 µm nitrocellulose membranes as per
195 manufacturer's instructions. Membranes were subsequently blocked for 1 hour at room
196 temperature in blocking buffer (PBS with 5% skimmed milk powder (Sigma-Aldrich) and 0.1%
197 Tween), then blotted overnight at 4 °C with 2 primary antibodies, 1 µg/ml mouse anti-human CXCL8
198 (R&D Systems) and 1:1000 rabbit anti-ENWVQ. Membranes were washed in wash buffer (PBS with
199 0.05% Tween) and incubated with 1:7500 goat anti-rabbit IgG A680nm and 1:7500 goat anti-mouse
200 IgG A790nm for 1 hour at room temperature before being visualised on LiCor Odyssey Fc
201 (Invitrogen).

202 SpyCEP activity against LL-37 was assessed by an 16 hour, 37 °C incubation of 5.56 µM human LL-37
203 (R&D Systems) with SpyCEP constructs at a 1:10 molar ratio in favour of LL-37. Reactions were
204 stopped, separated and blotted onto 0.22 µM nitrocellulose as above and incubated overnight at 4°C
205 in blocking buffer supplemented with 2 µg/ml polyclonal sheep IgG anti-LL-37 (R&D Systems).
206 Membranes were washed in wash buffer (PBS with 0.05% Tween) and incubated in blocking solution
207 with rabbit anti-sheep IgG (Abcam) at 1:40,000 dilution for 1 hour at room temperature and
208 visualised on LiCor Odyssey Fc (Invitrogen).

209 **Enzyme linked immunosorbent assay**

210 Catalytic activities of SpyCEP constructs were measured through detection of remaining intact CXCL8
211 or CXCL1 substrate following incubation with SpyCEP by ELISA (R&D Systems human CXCL8 and
212 CXCL1 DuoSet ELISA) as per manufacturer's instructions. For cleavage time courses 50 pM or 100 pM

213 SpyCEP were incubated with an equal volume of 20 nM human CXCL8 and CXCL1 respectively (R&D
214 Systems) and incubated at room temperature for 30 minutes. Reactions were halted at defined
215 timepoints with the addition of concentration of Pefabloc (Sigma-Aldrich) to a final concentration of
216 2 mg/ml (8.34 mM).

217 Linear regression analyses of the initial five time points of CXCL1 and CXCL8 cleavage (0, 1, 2, 3 and 4
218 minutes) was utlised to determine the maximal rate of SpyCEP activity.

219 **Mass spectrometry analysis of CXCL8 cleavage**

220 Analysis of CXCL8 cleavage was assayed on a SCIEX API6500 triple quadrupole electrospray mass
221 spectrometer coupled to a high-throughput robotic sample preparation and injection system,
222 RapidFire200 (Agilent Technologies). CXCL8 substrate, the 13 amino acid CXCL8 SpyCEP cleavage
223 product RVVEKFLKRAENS, and a heavy atom substituted internal standard of CXCL8 SpyCEP cleavage
224 product RV[U$_{13}$C$_{5}$ $_{15}$N-VAL]-EKF-[U-$_{13}$C$_{6}$ $_{15}$N-Leu]- KRAENS) were monitored by mass spectrometry. The
225 mass spectrometer was operated in positive electrospray MRM mode, and transitions (Q1/Q3) for
226 each species were optimised to give m/z as follows: CXCL8, 1048.7/615.3, CXCL8 cleavage product
227 526.2/211.1, internal standard 530.5/211.1. A dwell time of 50 ms was used for the MRM
228 transitions. The mass spectrometer was operated with a spray voltage of 5500 V and at a source
229 temperature of 650 °C.

230 To assay CXCL8 cleavage dynamically, chemokine and SpyCEP constructs were loaded into a 384 well
231 plate to the following final concentrations: 6.25-2000nM chemokine, 250 pM SpyCEP or 40 nM C-
232 terminal SpyCEP. Reactions were stopped at desired time points, 0-240 minutes, by the addition of
233 stop solution (1% formic acid) supplemented with 1 µM heavy atom substituted CXCL8 internal
234 standard and centrifuged 2000 xg for 10 minutes. Assay plates were transferred onto the
235 RapidFire200 integrated to the API6500 mass spectrometer. Samples were aspirated under vacuum
236 directly from 384-well assay plates for 0.6 s. The samples were then loaded onto a C18 solid-phase
237 extraction cartridge to remove non-volatile buffer salts, using HPLC -grade water supplemented with

238 0.1% (v/v) formic acid at a flow rate of 1.5 mL/min for 4 s. The retained analytes were eluted to the
239 mass spectrometer by washing the cartridge with acetonitrile HPLC-grade water (8:2, v/v) with 0.1%
240 (v/v) formic acid at 1.25 mL/min for 4 s. The cartridge was re-equilibrated with HPLC-grade water
241 supplemented with 0.1% (v/v) formic acid for 0.6 s at 1.5 mL/min. Results were normalised to the
242 fixed internal standard and converted to molarity by interpolation from a standard curve of known
243 cleaved CXCL8 concentrations.

244 **Kinetic analysis**

245 Linear regression analyses of the initial five time points of full length SpyCEP (0, 1, 2, 3, 4 minutes)
246 and C-terminal SpyCEP (0, 15, 30, 45, 60 minutes) CXCL8 reactions were plotted against substrate
247 concentration and kinetics derived from the Michaelis-Menton equation $Y = V_{max}*X/(K_M + X)$ and the
248 K_{cat} equation $Y = ET*k_{cat}*X/(K_M + X)$ where Et = enzyme concentration as fitted by Prism 8.0.2
249 (GraphPad).

250

251 **Results**
252

253 **Screening of human CXCL8 cleavage activity using fluorescent western blotting**
254

255 To initially assess the activity of our recombinant SpyCEP constructs we screened them for CXCL8
256 cleavage activity using two-colour multiplex western blotting. Human CXCL8 was incubated for 2
257 hours at 37 ^{o}C with SpyCEP constructs, the reaction products were separated by SDS-PAGE and
258 immunoblotted using seperate antibodies that detect either intact or cleaved CXCL8. Detection of
259 full-length CXCL8 (8 kDa, green bands) or the CXCL8 neo epitope (ENWVQ), exposed after SpyCEP
260 cleavage, (6 kDa, red bands) was evident with this system (Figure 1). Both native *S. pyogenes* SpyCEP
261 and recombinant full-length SpyCEP successfully cleaved CXCL8 to completion (Figure 1). As
262 expected, no cleavage was observed when using the catalytically dead mutant, SpyCEP^{DASA}. As has
263 been previously reported (Zingaretti et al., 2010), the SpyCEP N- and C-termini, when independently
264 expressed and purified, can be re-associated to form an active enzyme, which successfully cleaved
265 CXCL8. The N-terminal fragment of SpyCEP alone could not cleave CXCL8. Unexpectedly however,
266 the C-terminal fragment of SpyCEP was able to cleave CXCL8, albeit not to completion. This
267 independent catalytic activity was negated by mutation of the catalytic S617 to alanine (C-terminal^{SA}
268 construct, Figure 1). Cleavage of CXCL8 by the SpyCEP C-terminal fragment was enhanced when re-
269 associated with the catalytically inert N-terminal mutant (N-terminal^{DA} construct); indeed, activity
270 was equivalent to that observed with the re-associated enzyme under these conditions, with
271 cleavage of CXCL8 to near completion. However, the N-terminal^{DA} construct was unable to restore
272 catalytic activity to the C-terminal^{SA} construct when the two were combined.

273 The results demonstrated for the first time that the SpyCEP C-terminal fragment alone is sufficient
274 for catalytic cleavage of CXCL8 in this assay system. The data also established that, although the
275 presence of the SpyCEP N-terminal fragment enhanced enzymatic activity, the N-terminal residue
276 D151 was dispensable for enzymatic activity. We further sought to examine whether the C-terminal

277 displayed activity against the newly described substrate, LL-37 (Biswas et al., 2021). Western blot
278 analysis confirmed cleavage of LL-37 by full-length recombinant SpyCEP, demonstrated by a
279 reduction in band size, however the C-terminal fragment was unable to cleave LL-37 despite a high
280 molar ratio of enzyme to LL-37 (1: 10) and a prolonged 16-hour incubation at 37 °C (Figure EV1).

281

282 **Figure 1. Cleavage activity of recombinant SpyCEP constructs assayed by immunoblot.** Two colour
283 immunoblot showing cleavage of 150 ng CXCL8 incubated for 2 hours at 37 °C either alone (2nd lane)
284 or with panel of SpyCEP constructs at a 1:50 molar ratio (SpyCEP:CXCL8). Green bands represent
285 intact CXCL8 (anti-CXCL8 antibody); red bands represent cleaved CXCL8 (anti- ENWVQ). A 17 kDa
286 molecular weight marker is shown in blue, 8 kDa and 6 kDa molecular weights are highlighted by
287 arrows. Figure is representative of 2 independent immunoblots.

288

289 **Differntial cleavage of CXCL8 and CXCL1 by full-length and C-terminal SpyCEP**
290

291 To determine whether the catalytic activity of the C-terminal SpyCEP fragment was reproducible
292 over a shorter incubation period, we assessed CXCL8 cleavage by ELISA, where CXCL8 cleavage is
293 detected through a reduction in substrate concentration. SpyCEP C-terminal constructs were
294 incubated with CXCL8 at molar ratios ranging from 1:5 – 1:250 (enzyme: chemokine) over a 60
295 minute timecourse at room temperature. Full-length recombinant SpyCEP and the inactive C-
296 terminal fragment, C-terminal^{SA}, were included as controls at a molar ratio of 1:1000 and 1:5,
297 respectively. Under these conditions, near complete CXCL8 cleavage was observed for full-length
298 SpyCEP and a dose-dependent increase in catalytic activity was observed for the C-terminal fragment
299 (Figure 2). After 5 minutes incubation full-length SpyCEP cleaved over 50% of the starting CXCL8
300 input, with only 6.25% of CXCL8 remaining after 1 hour. At the highest concentration of C-terminal
301 SpyCEP tested, a 1:5 molar ratio, the C-terminal fragment alone cleaved 9% of the starting CXCL8 by
302 5 minutes, 25% by 30 minutes and 42% by 60 minutes. Indeed, at the lowest concentration tested, a
303 1:250 molar ratio, the C-terminal of SpyCEP cleaved 9% of CXCL8 input by 1 hour. As demonstrated
304 by immunofluorescent western blotting, the serine residue at position 617 was vital for SpyCEP
305 catalytic function as no CXCL8 cleavage was observed using the C-terminal^{SA} construct, even when

306 employed at the highest enzyme: chemokine ratio. After a 1 hour incubation, full length SpyCEP and
307 C-terminal contructs (assayed using a molar enzyme: chemokine ratio of 1:5, 1:25 and 1:50) cleaved
308 significantly more CXCL8 compared to the C-terminal^{SA} construct.

309 **Figure 2. Cleavage activity of SpyCEP and C-terminal SpyCEP$^{245-1613}$ constructs using CXCL8 ELISA.**
310 SpyCEP constructs were co-incubated with CXCL8. Graphs show residual CXCL8 after a 60-minute
311 room temperature incubation, using full length SpyCEP at a 1:1000 ratio to CXCL8; C-terminal at 1:5
312 – 1:250 molar ratio to CXCL8; and C-terminal S617A mutant at a 1:5 molar ratio to CXCL8. Reactions
313 were halted at specified timepoints by the addition of Pefabloc to a final concentration of 2 mg/ml.
314 N=6 experimental replicates for each construct, data points show means, error bars represent SD. ns
315 $p > 0.05$, * $p \leq 0.05$, **** $p \leq 0.0001$, at 60 minutes as determined by ordinary one-way ANOVA.

316

317 Further SDS-PAGE analysis of the catalytic activity of the C-terminal SpyCEP construct additionally
318 showed that C-terminal activity was not restricted to the CXCL8 substrate. Over 2 hours at 37 ^{o}C
319 using a 1:5 molar ratio of enzyme: substrate, the SpyCEP C-terminal construct was capable of
320 cleaving human CXCL1 to near completion (Figure EV2).

321 To further assess the activity of SpyCEP and to interrogate reaction rates against separate
322 chemokines, full-length SpyCEP was incubated with CXCL1 and CXCL8 and the remaining chemokine
323 levels determined by ELISA. Human CXCL1 or human CXCL8 were incubated with SpyCEP over a 30
324 minute, room temperature timecourse, at 1:200 or 1:400 molar ratios respectively (enzyme:
325 chemokine). When incubated in equal volumes, 50 pM SpyCEP rapidly and efficiently cleaved 20 nM
326 CXCL8, with ~ 15% of the chemokine input remaining after 10 minutes of incubation (Figure 3A). This
327 contrasted with CXCL1 cleavage, that required 100 pM SpyCEP to cleave just 25% of the chemokine
328 input over the same 10-minute period. Indeed, by 30 minutes SpyCEP had yet to cleave half of the
329 starting CXCL1 (Figure 3B). Utilising a linear regression of the initial 5 timepoints, where SpyCEP
330 activity is maximal, we found that 5 fmol of SpyCEP was able to cleave 284 fmol of CXCL8 per
331 minute, and 10 fmol of SpyCEP was capable of cleaving 62 fmol of CXCL1 per minute. These data
332 confirmed the activity of recombinant SpyCEP and highlighted differential cleavage efficiency across
333 the CXC substrate range – a feature which has been previously recognised but not quantified
334 (Goldblatt et al., 2019).

335

336 **Figure 3. Cleavage of CXCL8 and CXCL1 by recombinant full length SpyCEP.** 30-minute, room
337 temperature cleavage time course of: A. 20nM CXCL8 by an equal volume of 50pM SpyCEP and B.
338 20nM CXCL1 by an equal volume of 100pM SpyCEP. Cleavage reactions were halted at specified
339 timepoints by the addition of Pefabloc to a final concentration of 2 mg/ml and the remaining
340 chemokine measured by ELISA. N=6 experimental replicates for each data point, error bars represent
341 SD of mean values.

342

343 **Mass spectrometry-derived kinetics of active SpyCEP constructs**

344

345 To directly compare the active full-length and C-terminal SpyCEP constructs and to understand
346 relative catalytic efficiencies, a mass spectrometry approach to continuously assay the generation of
347 the 13 amino acid peptide cleaved from the native substrate CXCL8, following incubation with
348 enzyme, was employed. A range of CXCL8 concentrations (6.25-2000 nM) were incubated with a
349 fixed concentration of enzyme, either 250 pM for SpyCEP or 40 nM for the C-terminal SpyCEP$^{245\text{-}1613}$
350 and the production of the 13 amino acid peptide monitored over time. 250 pM full length SpyCEP
351 cleaved CXCL8 to near completion over 30 minutes when substrate concentrations were less than
352 250 nM; incomplete CXCL8 cleavage was observed when substrate concentration was in excess of
353 250 nM (Figure EV3A. In contrast, 40 nM of the C-terminal SpyCEP$^{245\text{-}\mathbf{1613}}$ cleaved CXCL8 to near
354 completion over 4 hours when the CXCL8 concentration was 250 nM or less; incomplete CXCL8
355 cleavage was again observed when substrate concentration were over 250 nM (Figure EV3B). Under
356 these conditions the C-terminal SpyCEP fragment maintained measurable catalytic activity
357 thoughout, though with reduced efficacy compared to the full-length construct. A 160-fold increase
358 in enzyme concentration and additional 3.5 hours reaction time were required to cleave a
359 comparable amount of CXCL8.

360 Linear regression analyses of the initial 5 time points, where the rate of cleaved CXCL8 production
361 was linear, were used to derive Michaelis-Menton plots (Figure 4) and K_M and K_{cat} values for each
362 construct (Table 2).

363

364

365 **Figure 4. Michaelis-Menton analysis of full length and C-terminal SpyCEP construct cleavage of**
366 **CXCL8.** Data points represent the mean change in cleaved CXCL8 production over time (M s^{-1}) of, **A.**
367 full-length SpyCEP and **B.** C-terminal SpyCEP). Error bars represent the standard error of the mean of
368 5 reactions.

369

370

371 **Table 2. Kinetic parameters of full length and C-terminal SpyCEP construct activity in cleavage of**
372 **CXCL8**

373 K_{cat} and K_M ± SD and K_{cat} / K_M for full length SpyCEP and C-terminal SpyCEP derived from Michaelis-
374 Menton graphs $Y = V_{max}*X/(K_M + X)$ and K_{cat} equation $Y = ET*k_{cat}*X/(K_M + X)$ where Et = enzyme
375 concentration, 2.5 $x10^{-10}$ for full length SpyCEP and 4 $x10^{-8}$ for C-terminal SpyCEP

376

377 K_M values for full length SpyCEP and the C-terminal fragment were 53.49 nM and 40.98 nM
378 respectively, suggesting nanomolar affinity of the SpyCEP constructs for CXCL8. The similarity in the
379 K_M values between the C- terminal SpyCEP fragment and the full-length enzyme point to a similar
380 ability to bind substrate. The K_{cat} values (indicative of the number of molecules of cleaved CXCL8
381 produced per second) however, differed substantially. The full length enzyme cleaved 1.34
382 molecules of CXCL8 per second compared to the C-terminal construct which cleaved 2.45 molecules
383 per hour, a 1,970-fold reduction in activity.

384

385 **Discussion**
386

387 SpyCEP is a serine protease and a leading virulence factor of *S. pyogenes,* with a narrow range of
388 substrate specificity, restricted to the family of ELR^+ CXC chemokines which modulate neutrophil
389 mediated immune responses and the newly identified substrate, LL-37 (Biswas et al., 2021).
390 Autocatalytic processing of SpyCEP results in the generation of two individual fragments that re-
391 assemble to form an active enzyme (Zingaretti et al., 2010). Here, we describe the enzyme kinetics of
392 full-length SpyCEP and report the K_M of the enzyme for its natural substrate to be remarkably low,
393 just 53.49 nM, consistent with high efficiency. Furthermore, we demonstrate that the C-terminal
394 SpyCEP fragment can catalyse the cleavage of CXCL1 and CXCL8 independent of the N-terminal
395 fragment. Indeed, when K_M values were compared, they were found to be similar, suggesting that
396 substrate binding may be confined to the C-terminal domain of SpyCEP. The enzymatic activity of the
397 C-terminal SpyCEP fragment was, however, markedly reduced compared to full-length SpyCEP. The
398 N-terminal and N-terminal^{DA} constructs were equally able to restore full catalytic activity of the C-
399 terminal SpyCEP fragment. Collectively, this suggests that although the aspartate 151 of the N-
400 terminal fragment may be dispensable for catalysis, the domain itself is important for optimal
401 enzyme activity.

402 Serine proteases are ubiquitous and comprise up to one third of all proteolytic enzymes currently
403 described. They are currently categorised by the MEROPS database (Rawlings et al., 2012) into 13
404 distinct clans, being differentiated into groups of proteins based on their evolution from the same
405 common ancestor, with SpyCEP belonging to the S8 family of the SB clan. S8 serine proteases are
406 typified by a classical catalytic triad composed of serine, histidine and aspartic acid residues that
407 together contribute to the hydrolysis of a peptide bond within the substrate. It is recognised that a
408 number of serine protease clans employ a variation on the S8 catalytic triad, utilising instead a triad
409 of serine, histidine, and glutamic acid, or serine, glutamic acid, and aspartic acid residues. Other
410 clans utilise catalytic dyads of lysine and histidine or histidine and serine for proteolytic activity. Our

411 data suggest that SpyCEP activity can reside in a catalytic dyad of histidine and serine, albeit at a
412 reduced efficacy. It is likely this large gulf in efficiency explains the failure of previous studies to
413 detect catalytic activity within the isolated C-terminal SpyCEP fragment (Zingaretti et al., 2010).

414 Within serine proteases there are additional features, beyond the catalytic triad residues, which can
415 contribute to activity. The oxyanion hole for example, a pocket in the active site composed of
416 backbone amide NH groups, may provide substrate stabilisation and help drive catalysis (Hedstrom,
417 2002). Additional residues located in close proximity to the catalytic pocket can also mitigate a loss
418 of activity resulting from a missing residue, and water also has the potential to moonlight as a
419 missing functional group (Hedstrom, 2002). These 'stand ins' can provide a possible substitute
420 machinery to help drive catalytic function. Indeed, some studies have shown that, even with all
421 three catalytic triad residues removed, serine proteases are still capable of catalysis at rates 1000-
422 fold greater than the background rate of hydrolysis (Corey and Craik, 1992, Hedstrom, 2002, Paul
423 and James, 1988).

424 Mass spectrometry-based kinetics showed that full-length active SpyCEP has a K_M of 53.49 nM and
425 K_{cat} of 1.34 molecules per second; values which are in agreement with our initial ELISA-based kinetic
426 assessment (McKenna et al., 2020). In contrast, the C-terminal fragment of SpyCEP has a K_M of 40.98
427 nM and K_{cat} of 0.00068 molecules per second. These constructs both demonstrated low, nanomolar
428 K_M values, suggesting a high binding efficiency of SpyCEP for its natural substrate CXCL8, likely
429 conferred by the C-terminal domain. This is in keeping with the fact that low nanomolar
430 concentrations of CXCL8 are optimal for neutrophil recruitment (Goldblatt et al., 2019). Although K_M
431 values are often reported in the μM – mM range, nanomolar K_M values are not without precedent
432 for other serine proteases; human Kallikrein 6 has a reported K_M of 300 nM and Factor Xa, a
433 constituent of the prothrombinase complex, has a K_M of 150 nM for prothrombin (Angelo et al.,
434 2006, Luettgen et al., 2011). Enzyme specificity, a constant which measures the cleavage efficiency
435 of enzymes, (K_{cat} /K_M), for full length SpyCEP was estimated to be 2.46 x10^7 M^{-1} s^{-1}, a value in the

436 order of magnitude typical for serine proteases (Hedstrom, 2002). The specificity constant of the C-
437 terminal fragment was ~1500-fold less, 1.67 x10^4 M^{-1} s^{-1}, and K_{cat} ~2000 fold less, a reduction that is
438 in line with previously reported aspartic acid mutants from a systematic mutational study of the
439 *Bacillus amyloliquefaciens* subtilisin catalytic triad (Paul and James, 1988).

440 The kinetic assays attributed a marked increase in CXCL8 turnover to the additional presence of the
441 N-terminal fragment. Although we did not specifically evaluate the role of the aspartate residue at
442 position 151 on the kinetics of SpyCEP activity, this residue did not contribute appreciably to
443 cleavage of CXCL8 when evaluated using immunoblotting. This raises a question as to whether the N-
444 terminal fragment confers some additional structural contribution to enzyme activity. Our data
445 strongly suggest that substrate binding is likely to be attributed to the C-terminal fragment, a finding
446 consistent with related cell envelope proteinases of *Lactococc*i (Siezen, 1999) and the closely related
447 streptococcal protein, C5a peptidase (Kagawa et al., 2009).

448 The implications of our findings relating to activity of the C-terminal SpyCEP fragment in *S. pyogenes*
449 pathogenesis are currently unclear; without the N-terminus, the enzymatic activity detected may be
450 too low to be of consequence for chemokine cleavage *in vivo,* and in nature both N- and C-terminal
451 fragments are likely to co-exist. SpyCEP has been the focus of *S. pyogenes* vaccine development
452 since 2006 (Rodriguez-Ortega et al., 2006), used either in isolation or combination with other
453 antigenic targets (Bensi et al., 2012, McKenna et al., 2020, Pandey et al., 2016, Reglinski et al., 2016,
454 Rivera-Hernandez et al., 2016). Vaccine-induced SpyCEP specific antibodies appear not to act
455 through traditional opsonic means (Rivera-Hernandez et al., 2019) and so likely act through
456 inhibition of SpyCEP activity. A majority of vaccine preparations evaluated have been based on
457 'CEP5'; a polypeptide spanning residues 35 – 587 of SpyCEP which contains the N- terminal fragment
458 and only part of the C terminal fragment (Turner et al., 2009b). Our findings relating to enzyme
459 function highlight the possibility that antibodies targeting the C-terminal fragment of SpyCEP are
460 more likely to provide greater neutralizing activity, and potentially improve vaccine efficacy.

461 **Funding**

462 This work was funded by a Biotechnology and Biological Sciences Research Council (BBSRC) NPIF
463 iCASE studentship (MP) and a Wellcome Trust Collaborative award 215539: 'Understanding and
464 exploiting Group A streptococcal anti-chemotactic proteases in vaccines for infection' (SS and JP).

465

466 **Acknowledgements**
467 The authors are grateful for the support of a GSK Golden Triangle Discovery Partnership in Academia
468 Collaboration (DPAC) that permitted development of the mass spectrometry high throughput
469 cleavage assay and reagent provision. SS acknowledges the Imperial College London NIHR
470 Biomedical Research Centre.

471 **Author contributions**
472 MP, CH, AF, DM, JP and SS designed the study. MP, CH, MR, RJE, RAL collected the data. MP and CH
473 analysed the data. MP, CH, AF, DM, JP and SS interpreted the data. MP collected and prepared the
474 figures. MP, MR, JP and SS drafted the manuscript. MP, CH, AF, MR, RJE, RAL, DM, JP, SS, revised the
475 manuscript content.

476 **Conflict of interest**
477 All authors declare there is no conflict of interest.

478
479
480
481
482
483
484
485
486
487
488

489 **Expanded View figures**
490

491

492 **Figure EV1. Western blot of SpyCEP specific LL3-7 cleavage.** Immunoblot of 500 ng human LL-37
493 incubated for 16 hours at 37 °C either alone (lane 7) or with a panel of SpyCEP constructs at a 10:1
494 molar ratio in favour of LL-37. 4.5 kDa full length LL-37 band and 3.5 kDa cleaved LL-37 band are
495 indicated by arrows and were detected with 2 µg/ml sheep IgG polyclonal LL-37 antibody and rabbit
496 anti-sheep IgG antibody (1:40,000). Figure is representative of two experiments.

497

498 **Figure EV2. Comparative cleavage of CXCL1 and CXCL8 by C-terminal SpyCEP.** SDS-page analysis of
499 A. 5 µM human CXCL1 (all lanes) or B. 5 µM human CXCL8 (all lanes) cleavage by C-terminal SpyCEP
500 at a 1:5 – 1:5000 molar ratio (SpyCEP: Chemokine). SpyCEP^{DASA}, C-terminal^{SA} and N-terminal controls
501 were all assayed at the highest 1:5 molar ratio.

502

503 **Figure EV3. CXCL8 cleavage by active recombinant SpyCEP constructs using mass spectrometry**.

504 **A.** Production of the 13 amino acid species cleaved from CXCL8 by 250 pM of full length SpyCEP over
505 30 minutes at room temperature, following incubation with 6.25 nM – 2000 nM CXCL8, 1: 250 –
506 8000 molar ratio (SpyCEP: CXCL8). **B**. Production of the 13 amino acid species by 40 nM SpyCEP C-
507 terminal fragment over a 4 hour room temperature incubation, following incubation with 6.25 nM –
508 2000 nM CXCL8, 1: 0.15 – 50 molar ratio (SpyCEP: CXCL8). N=5 experimental replicates per data
509 point, error bars represent SD. Figure is representative of two experiments

510

511

512

513

514

515

516

517

518

519

520

521

522

523

524

525 **References**

526 ABATE, F., MALITO, E., FALUGI, F., MARGARIT, Y. R. I. & BOTTOMLEY, M. J. 2013. Cloning,
527 expression, purification, crystallization and preliminary X-ray diffraction analysis of
528 SpyCEP, a candidate antigen for a vaccine against Streptococcus pyogenes. *Acta*
529 *Crystallogr Sect F Struct Biol Cryst Commun,* 69**,** 1103-6.
530 ANGELO, P. F., LIMA, A. R., ALVES, F. M., BLABER, S. I., SCARISBRICK, I. A., BLABER, M.,
531 JULIANO, L. & JULIANO, M. A. 2006. Substrate specificity of human kallikrein 6: salt
532 and glycosaminoglycan activation effects. *J Biol Chem,* 281**,** 3116-26.
533 BENSI, G., MORA, M., TUSCANO, G., BIAGINI, M., CHIAROT, E., BOMBACI, M., CAPO, S.,
534 FALUGI, F., MANETTI, A. G., DONATO, P., SWENNEN, E., GALLOTTA, M., GARIBALDI,
535 M., PINTO, V., CHIAPPINI, N., MUSSER, J. M., JANULCZYK, R., MARIANI, M.,
536 SCARSELLI, M., TELFORD, J. L., GRIFANTINI, R., NORAIS, N., MARGARIT, I. & GRANDI,
537 G. 2012. Multi high-throughput approach for highly selective identification of vaccine
538 candidates: the Group A Streptococcus case. *Mol Cell Proteomics,* 11**,** M111.015693.
539 BISWAS, D., AMBALAVANAN, P., RAVINS, M., ANAND, A., SHARMA, A., LIM, K. X. Z., TAN, R.
540 Y. M., LIM, H. Y., SOL, A., BACHRACH, G., ANGELI, V. & HANSKI, E. 2021. LL-37-
541 mediated activation of host receptors is critical for defense against group A
542 streptococcal infection. *Cell Rep,* 34**,** 108766.
543 CARAPETIS, J. R., STEER, A. C., MULHOLLAND, E. K. & WEBER, M. 2005. The global burden of
544 group A streptococcal diseases. *Lancet Infect Dis,* 5**,** 685-94.
545 COREY, D. R. & CRAIK, C. S. 1992. An investigation into the minimum requirements for
546 peptide hydrolysis by mutation of the catalytic triad of trypsin. *Journal of the*
547 *American Chemical Society,* 114**,** 1784-1790.
548 EDWARDS, R. J., TAYLOR, G. W., FERGUSON, M., MURRAY, S., RENDELL, N., WRIGLEY, A., BAI,
549 Z., BOYLE, J., FINNEY, S. J., JONES, A., RUSSELL, H. H., TURNER, C., COHEN, J.,
550 FAULKNER, L. & SRISKANDAN, S. 2005. Specific C-terminal cleavage and inactivation
551 of interleukin-8 by invasive disease isolates of Streptococcus pyogenes. *J Infect Dis,*
552 192**,** 783-90.
553 EDWARDS, R. J., WRIGLEY, A., BAI, Z., BATEMAN, M., RUSSELL, H., MURRAY, S., LU, H.,
554 TAYLOR, G. W., BOOBIS, A. R. & SRISKANDAN, S. 2007. C-terminal antibodies (CTAbs):
555 a simple and broadly applicable approach for the rapid generation of protein-specific
556 antibodies with predefined specificity. *Proteomics,* 7**,** 1364-72.
557 GOLDBLATT, J., LAWRENSON, R. A., MUIR, L., DATTANI, S., HOFFLAND, A., TSUCHIYA, T.,
558 KANEGASAKI, S., SRISKANDAN, S. & PEASE, J. E. 2019. A Requirement for Neutrophil
559 Glycosaminoglycans in Chemokine:Receptor Interactions Is Revealed by the
560 Streptococcal Protease SpyCEP. *J Immunol,* 202**,** 3246-3255.
561 HEDSTROM, L. 2002. Serine Protease Mechanism and Specificity. *Chemical Reviews,* 102**,**
562 4501-4524.
563 JOBICHEN, C., TAN, Y. C., PRABHAKAR, M. T., NAYAK, D., BISWAS, D., PANNU, N. S., HANSKI,
564 E. & SIVARAMAN, J. 2018. Structure of ScpC, a virulence protease from
565 Streptococcus pyogenes, reveals the functional domains and maturation mechanism.
566 *Biochem J,* 475**,** 2847-2860.
567 KAGAWA, T. F., O'CONNELL, M. R., MOUAT, P., PAOLI, M., O'TOOLE, P. W. & COONEY, J. C.
568 2009. Model for substrate interactions in C5a peptidase from Streptococcus
569 pyogenes: A 1.9 A crystal structure of the active form of ScpA. *J Mol Biol,* 386**,** 754-
570 72.

571 KAUR, S. J., NERLICH, A., BERGMANN, S., ROHDE, M., FULDE, M., ZAHNER, D., HANSKI, E.,
572 ZINKERNAGEL, A., NIZET, V., CHHATWAL, G. S. & TALAY, S. R. 2010. The CXC
573 chemokine-degrading protease SpyCep of Streptococcus pyogenes promotes its
574 uptake into endothelial cells. *J Biol Chem,* 285**,** 27798-805.
575 KURUPATI, P., TURNER, C. E., TZIONA, I., LAWRENSON, R. A., ALAM, F. M., NOHADANI, M.,
576 STAMP, G. W., ZINKERNAGEL, A. S., NIZET, V., EDWARDS, R. J. & SRISKANDAN, S.
577 2010. Chemokine-cleaving Streptococcus pyogenes protease SpyCEP is necessary
578 and sufficient for bacterial dissemination within soft tissues and the respiratory
579 tract. *Mol Microbiol,* 76**,** 1387-97.
580 LUETTGEN, J. M., KNABB, R. M., HE, K., PINTO, D. J. P. & RENDINA, A. R. 2011. Apixaban
581 inhibition of factor Xa: Microscopic rate constants and inhibition mechanism in
582 purified protein systems and in human plasma. *Journal of Enzyme Inhibition and*
583 *Medicinal Chemistry,* 26**,** 514-526.
584 LYNSKEY, N. N., GOULDING, D., GIERULA, M., TURNER, C. E., DOUGAN, G., EDWARDS, R. J. &
585 SRISKANDAN, S. 2013. RocA Truncation Underpins Hyper-Encapsulation, Carriage
586 Longevity and Transmissibility of Serotype M18 Group A Streptococci. *PLOS*
587 *Pathogens,* 9**,** e1003842.
588 MCKENNA, S., MALITO, E., ROUSE, S. L., ABATE, F., BENSI, G., CHIAROT, E., MICOLI, F.,
589 MANCINI, F., GOMES MORIEL, D., GRANDI, G., MOSSAKOWSKA, D., PEARSON, M.,
590 XU, Y., PEASE, J., SRISKANDAN, S., MARGARIT, I., BOTTOMLEY, M. J. & MATTHEWS, S.
591 2020. Structure, dynamics and immunogenicity of a catalytically inactive CXC
592 chemokine-degrading protease SpyCEP from Streptococcus pyogenes.
593 *Computational and Structural Biotechnology Journal,* 18**,** 650-660.
594 MIDDLETON, J., NEIL, S., WINTLE, J., CLARK-LEWIS, I., MOORE, H., LAM, C., AUER, M., HUB, E.
595 & ROT, A. 1997. Transcytosis and surface presentation of IL-8 by venular endothelial
596 cells. *Cell,* 91**,** 385-95.
597 PANDEY, M., LANGSHAW, E., HARTAS, J., LAM, A., BATZLOFF, M. R. & GOOD, M. F. 2015. A
598 synthetic M protein peptide synergizes with a CXC chemokine protease to induce
599 vaccine-mediated protection against virulent streptococcal pyoderma and
600 bacteremia. *J Immunol,* 194**,** 5915-25.
601 PANDEY, M., MORTENSEN, R., CALCUTT, A., POWELL, J., BATZLOFF, M. R., DIETRICH, J. &
602 GOOD, M. F. 2016. Combinatorial Synthetic Peptide Vaccine Strategy Protects
603 against Hypervirulent CovR/S Mutant Streptococci. *J Immunol,* 196**,** 3364-74.
604 PAUL, C. & JAMES, A. W. 1988. Dissecting the catalytic triad of a serine protease. *Nature,*
605 332**,** 564.
606 RALPH, A. P. & CARAPETIS, J. R. 2013. Group a streptococcal diseases and their global
607 burden. *Curr Top Microbiol Immunol,* 368**,** 1-27.
608 RAWLINGS, N. D., BARRETT, A. J. & BATEMAN, A. 2012. MEROPS: the database of proteolytic
609 enzymes, their substrates and inhibitors. *Nucleic acids research,* 40**,** D343-D350.
610 REGLINSKI, M., LYNSKEY, N. N., CHOI, Y. J., EDWARDS, R. J. & SRISKANDAN, S. 2016.
611 Development of a multicomponent vaccine for Streptococcus pyogenes based on the
612 antigenic targets of IVIG. *J Infect,* 72**,** 450-9.
613 RIVERA-HERNANDEZ, T., CARNATHAN, D. G., JONES, S., CORK, A. J., DAVIES, M. R., MOYLE, P.
614 M., TOTH, I., BATZLOFF, M. R., MCCARTHY, J., NIZET, V., GOLDBLATT, D., SILVESTRI,
615 G. & WALKER, M. J. 2019. An Experimental Group A Streptococcus Vaccine That
616 Reduces Pharyngitis and Tonsillitis in a Nonhuman Primate Model. *MBio,* 10.

RIVERA-HERNANDEZ, T., PANDEY, M., HENNINGHAM, A., COLE, J., CHOUDHURY, B., CORK, A. J., GILLEN, C. M., GHAFFAR, K. A., WEST, N. P., SILVESTRI, G., GOOD, M. F., MOYLE, P. M., TOTH, I., NIZET, V., BATZLOFF, M. R. & WALKER, M. J. 2016. Differing Efficacies of Lead Group A Streptococcal Vaccine Candidates and Full-Length M Protein in Cutaneous and Invasive Disease Models. *MBio,* 7.

RODRIGUEZ-ORTEGA, M. J., NORAIS, N., BENSI, G., LIBERATORI, S., CAPO, S., MORA, M., SCARSELLI, M., DORO, F., FERRARI, G., GARAGUSO, I., MAGGI, T., NEUMANN, A., COVRE, A., TELFORD, J. L. & GRANDI, G. 2006. Characterization and identification of vaccine candidate proteins through analysis of the group A Streptococcus surface proteome. *Nat Biotechnol,* 24**,** 191-7.

SIEZEN, R. J. 1999. Multi-domain, cell-envelope proteinases of lactic acid bacteria. *Antonie Van Leeuwenhoek,* 76**,** 139-55.

TURNER, C. E., KURUPATI, P., JONES, M. D., EDWARDS, R. J. & SRISKANDAN, S. 2009a. Emerging role of the interleukin-8 cleaving enzyme SpyCEP in clinical Streptococcus pyogenes infection. *J Infect Dis,* 200**,** 555-63.

TURNER, C. E., KURUPATI, P., WILES, S., EDWARDS, R. J. & SRISKANDAN, S. 2009b. Impact of immunization against SpyCEP during invasive disease with two streptococcal species: Streptococcus pyogenes and Streptococcus equi. *Vaccine,* 27**,** 4923-9.

ZINGARETTI, C., FALUGI, F., NARDI-DEI, V., PIETROCOLA, G., MARIANI, M., LIBERATORI, S., GALLOTTA, M., TONTINI, M., TANI, C., SPEZIALE, P., GRANDI, G. & MARGARIT, I. 2010. Streptococcus pyogenes SpyCEP: a chemokine-inactivating protease with unique structural and biochemical features. *Faseb j,* 24**,** 2839-48.

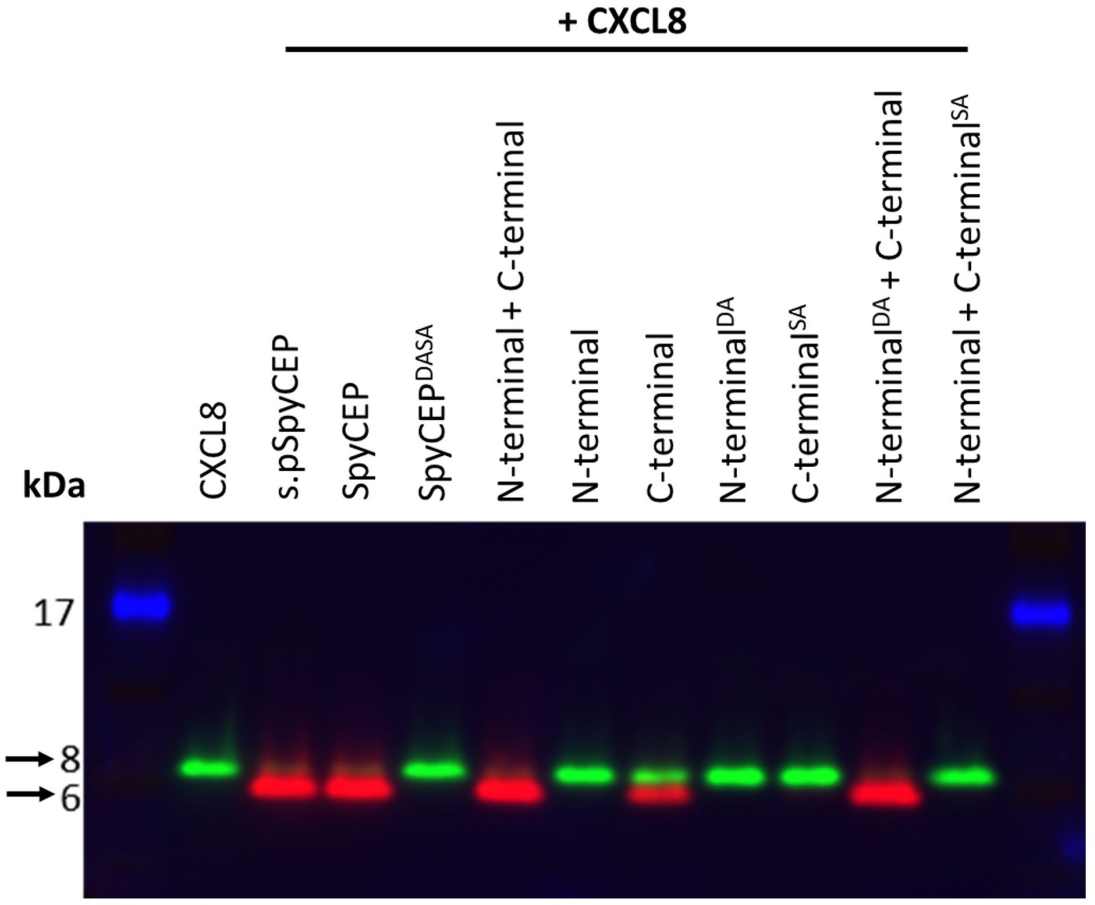

Figure 1. Cleavage activity of recombinant SpyCEP constructs assayed by immunoblot. Two colour immunoblot showing cleavage of 150 ng CXCL8 incubated for 2 hours at 37 °C either alone (2nd lane) or with panel of SpyCEP constructs at a 1:50 molar ratio (SpyCEP:CXCL8). Green bands represent intact CXCL8 (anti-CXCL8 antibody); red bands represent cleaved CXCL8 (anti-ENWVQ). A 17 kDa molecular weight marker is shown in blue, 8 kDa and 6 kDa molecular weights are highlighted by arrows. Figure is representative of 2 independent immunoblots.

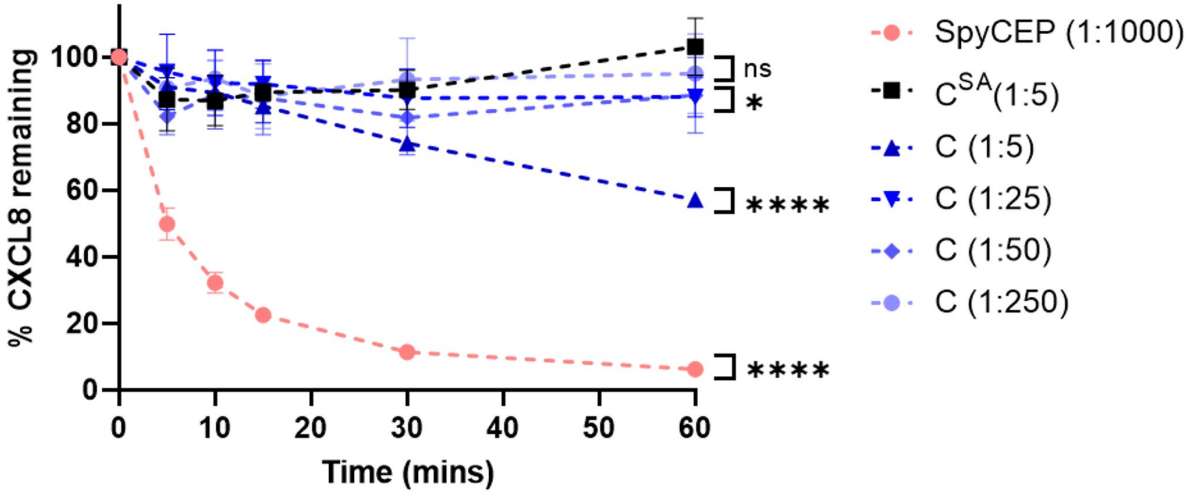

Figure 2. Cleavage activity of SpyCEP and C-terminal SpyCEP$^{245\text{-}1613}$ constructs using CXCL8 ELISA. SpyCEP constructs were co-incubated with CXCL8. Graphs show residual CXCL8 after a 60-minute room temperature incubation, using full length SpyCEP at a 1:1000 ratio to CXCL8; C-terminal at 1:5 – 1:250 molar ratio to CXCL8; and C-terminal S617A mutant at a 1:5 molar ratio to CXCL8. Reactions were halted at specified timepoints by the addition of Pefabloc to a final concentration of 2 mg/ml. N=6 experimental replicates for each construct, data points show means, error bars represent SD. ns $p > 0.05$, * $p \leq 0.05$, **** $p \leq 0.0001$, at 60 minutes as determined by ordinary one-way ANOVA.

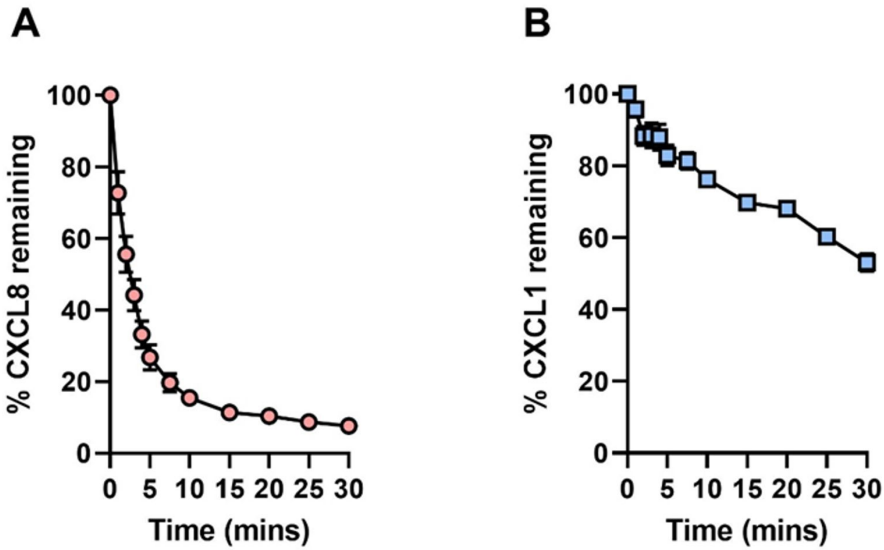

Figure 3. Cleavage of CXCL8 and CXCL1 by recombinant full length SpyCEP. 30-minute, room temperature cleavage time course of: A. 20nM CXCL8 by an equal volume of 50pM SpyCEP and B. 20nM CXCL1 by an equal volume of 100pM SpyCEP. Cleavage reactions were halted at specified timepoints by the addition of Pefabloc to a final concentration of 2 mg/ml and the remaining chemokine measured by ELISA. N=6 experimental replicates for each data point, error bars represent SD of mean values.

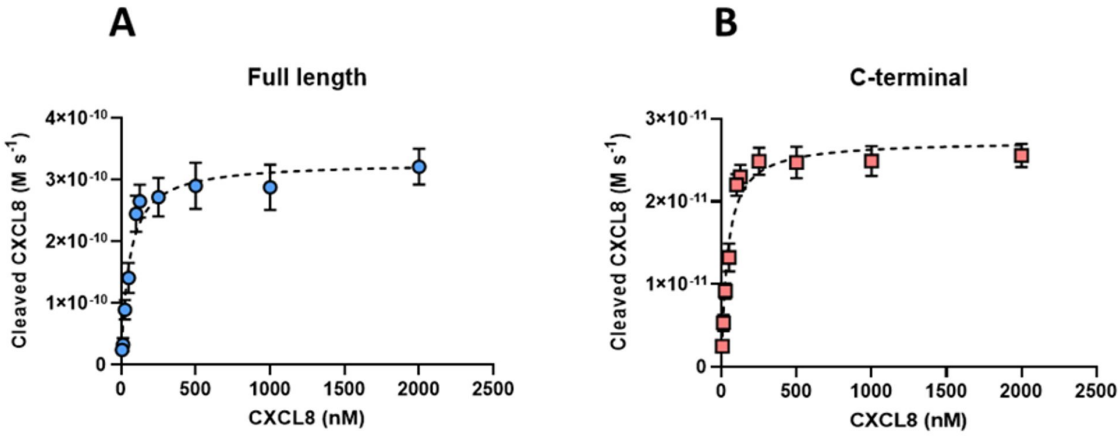

Figure 4. Michaelis-Menton analysis of full length and C-terminal SpyCEP construct cleavage of CXCL8. Data points represent the mean change in cleaved CXCL8 production over time (M s^{-1}) of, **A.** full-length SpyCEP and **B.** C-terminal SpyCEP). Error bars represent the standard error of the mean of 5 reactions.

SpyCEP construct	SpyCEP construct description
SpyCEP	Full-length, SpyCEP$^{34\text{-}1613}$-6His
SpyCEP^{DASA}	Full length double mutant, SpyCEP$^{34\text{-}1613\ D151A,\ S617A}$-6His
N-terminal (N)	N-terminal fragment, FLAG-TEV-SpyCEP$^{34\text{-}244}$
C-terminal (C)	C-terminal fragment, SpyCEP$^{245\text{-}1613}$-6His
N-terminal^{DA} (N^{DA})	N-terminal mutant fragment, FLAG-TEV-SpyCEP$^{34\text{-}244\ D151A}$
C-terminal^{SA} (C^{SA})	C-terminal mutant fragment, SpyCEP$^{245\text{-}1613\ S617A}$-6His
s.pSpyCEP	SpyCEP from *S. pyogenes* supernatant, SpyCEP$^{34\text{-}1613}$-6His

Table 1. SpyCEP constructs used in this study. Constructs were expressed recombinantly in *E. coli* except for s.pSpyCEP that was expressed in, and purified from *S. pyogenes*.

Construct	K_{cat} ± SD (s^{-1})	K_M ± SD (nM)	K_{cat}/K_M (M^{-1} s^{-1})
Full-length	1.34 ± 0.61	53.49 ± 10.36	2.46 x10^7
C-terminal	0.00068 ± 0.00003	40.98 ± 7.2	1.67 x10^4

Table 2. Kinetic parameters of full length and C-terminal SpyCEP construct activity in cleavage of CXCL8. K_{cat} and K_M ± SD and K_{cat} / K_M for full length SpyCEP and C-terminal SpyCEP derived from Michaelis-Menton graphs $Y = V_{max}*X/(K_M + X)$ and K_{cat} equation $Y = ET*k_{cat}*X/(K_M + X)$ where Et = enzyme concentration, 2.5 x10^{-10} for full length SpyCEP and 4 x10^{-8} for C-terminal SpyCEP